JOC Article

Electronic Effects in (salen)Mn-Based Epoxidation Catalysts

Luigi Cavallo and Heiko Jacobsen*,†

Department of Chemistry, Università di Salerno, Via Salvador Allende, Baronissi (SA) I-84081, Italy

jacobsen@kemkom.com

Received January 18, 2003

Presented are density functional calculations on various Mn(salen) systems that are active catalysts in the epoxidation of olefins. Correlation of various structural properties such as Mn=O bond strengths, atomic charges, and C−O distances of evolving bonds in transition state geometries with modified Hammett constants reveal a mechanistic picture of the epoxidation reaction, supporting previous experimental results. Enantioselectivity is tied to the position of a transition state along the reaction coordinate for the first C−O bond formation step, when an olefin is approaching the epoxidation catalyst. Electronic effects exhibited by the 5,5′ substituents of the salen ligand manifest themselves in a tuning of the Mn=O bond strength, which in turn influences the C−O distance of the forming bond in the transition state geometry.

Introduction

One of the most important methods of controlling the product specificity during epoxidation of conjugated olefins that has evolved during the past decade is the so-called Jacobsen−Katsuki epoxidation.[1] In this type of reaction, chiral (salen)Mn^{III} catalysts are employed to achieve high enantiomeric excess in the epoxidation products. The prototype for the (salen)Mn^{III} catalysts used in this reaction is Jacobsen's catalyst **1**, effective for virtual every class of conjugated olefins.

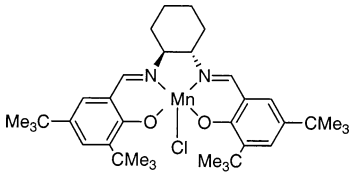

1

The mechanistic scheme that is commonly proposed for this type of oxygen transfer reaction consists of a two-step catalytic cycle. In a first step, an intermediate (salen)Mn^{V} oxo complex is generated,[2,3] which in a second step carries the activated oxygen to the olefinic double bond (Scheme 1).

SCHEME 1

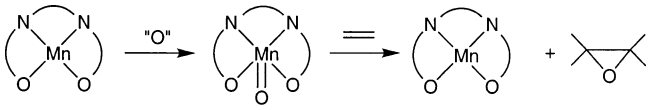

The first investigations of the (salen)Mn^{III}-catalyzed epoxidation established that steric bulk at the 3,3′ position of the salen ligand is essential in order to achieve high enantioselectivity.[4] However, soon after the initial report dramatic catalyst electronic influences on the enantioselectivity of (salen)Mn-catalyzed epoxidation of *cis*-disubstituted olefins were observed. Variations of the electronic properties of the substituents at the 5,5′ position have a profound effect on the enantioselectivity of the epoxidation reaction.[5] It was suggested that these effects might be interpreted according to a Hammond Postulate argument, wherein ligand substituents influence enantioselectivity by modulating the reactivity of the high-valent (salen)Mn^{V} oxo intermediate. Thus, electron-withdrawing substituents were proposed to lead to a more reactive (salen)Mn^{V} oxo intermediate, which adds to an olefin in a comparatively early transition state and affords lower levels of enantioselectivity. Conversely, electron-donating groups attenuate the reactivity of the oxo species, leading to a comparatively late transition state and concomitantly higher enantioselectivity. This suggested scenario is schematically depicted in Figure 1.

In a detailed mechanistic study, Jacobsen and coworkers present a wide range of experimental data supporting the proposition that the electronic character of chiral (salen)Mn catalysts influences the enantioselectivity of the catalytic epoxidation by altering the

† Current address: KemKom, 1864 Burfield Avenue, Ottawa, Ontario K1J 6T1, Canada.

(1) (a) Jacobsen, E. N. In *Catalytic Asymmetric Synthesis*; Ojima, I., Ed.; VCH: Weinheim, 1993; Chapter 4.2. (b) Jacobsen, E. N. In *Comprehensive Organometallic Chemistry II*; Wilkinson, G., Stone, F. G. A., Abel, E. W., Hegedus, L. S., Eds.; Pergamon: New York, 1995; Vol. 12 Chapter 11.1. (c) Katsuki, T. *Coord. Chem. Rev.* **1995**, *140*, 189. (d) Katsuki, T. *J. Mol. Catal. A* **1996**, *113*, 87. (e) Dalton, C. T.; Ryan, K. M.; Wall, V. M.; Bousquet, C.; Gilheany, D. G. *Top. Catal.* **1998**. *5*, 75. (f) Flessner, T.; Doye, S. *J. Prakt. Chem.* **1999**, *341*, 436. (g) Katsuki, T. *Adv. Synth. Catal.* **2002**, *344*, 131.

(2) Srinivasan, K.; Michaud, P.; Kochi, J. K. *J. Am. Chem. Soc.* **1986**, *108*, 2309.

(3) Feichtinger, D.; Plattner, D. A. *Angew. Chem.* **1997** *109*, 1796; *Angew. Chem., Int. Ed. Engl.* **1997**, *36*, 1718.

(4) Zhang, W.; Loebach, J. L.; Wilson, S. R.; Jacobsen, E. N. *J. Am. Chem. Soc.* **1990**, *112*, 2801.

(5) Jacobsen, E. N.; Zhang, W.; Güler, M. L. *J. Am. Chem. Soc.* **1991**, *113*, 6703.

10.1021/jo034059a CCC: $25.00
Published on Web 07/16/2003

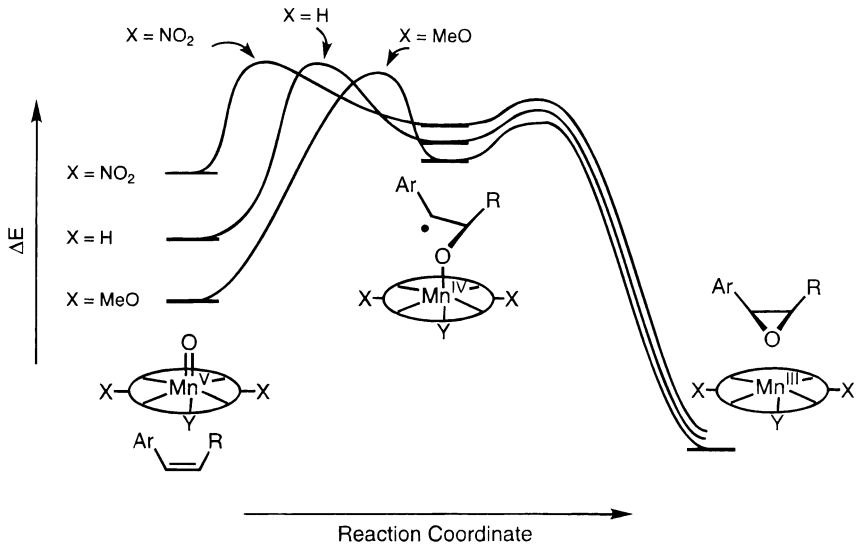

FIGURE 1. Schematic energy diagram illustrating the proposed effect of ligand substituents on the (salen)Mn-catalyzed epoxidation reaction, as proposed by Jacobsen. (Reprinted from ref 6 with permission of the author.)

position of the transition state in the first C−O bond-forming step.[6] Among the critical experimental results are linear Hammett plots correlating enantioselectivity in the epoxidation of *cis*-disubstituted olefins with Hammett substituent constants of the 5,5′-substituents on the salen ligand system of the catalyst.

Up to now, a variety of computational studies on the (salen)Mn-catalyzed epoxidation reaction have appeared in the literature,[7] often based on the model catalyst (acacen′)Mn^{III} **2** and the related oxo species (acacen′)Mn^{V} **3** (acacen′ = $^{-}O(CH)_3N\text{-}C_2H_4\text{-}N(CH)_3O^{-}$). Issues dealt with in these studies include reaction profiles, spin states, and the mechanism of enantioselectivity. In particular, in a previous study we suggested that the role of the functional group conjugated to the C=C double bond is to confer regioselectivity to the attack of the olefinic bond on the Mn=O group.[7e] However, the problem of catalyst tuning has not yet been addressed by computational approaches.

Here, we present the results of density functional calculations on the (salen)Mn^{III} complexes **2a**−**f** and the (salen)Mn^{V} oxo species **3a**−**f**, as well as on the model compounds **2** and **3**.

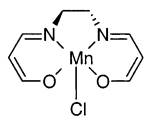

2

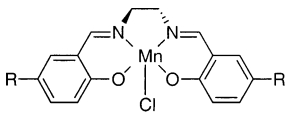

2a: R = H
2b: R = NO_2
2c: R = OMe
2d: R = CMe_3
2e: R = Cl
2f : R = Me

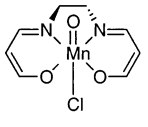

3

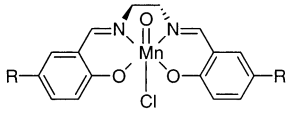

3a: R = H
3b: R = NO_2
3c: R = OMe
3d: R = CMe_3
3e: R = Cl
3f : R = Me

Two questions are at the center of the present work: Is it possible to correlate the results of density functional calculations on such extended systems with experimental data, and if so, what can be deduced on the role of the 5,5′-substituents in determining enantioselective discrimination? We will address these questions in detail, after presenting a concise account of the computational methodology employed in the current work.

Computational Details

Gradient corrected density functional calculations were carried out, with corrections for exchange and correlation according to Becke[8] and Perdew,[9] respectively (BP86). Recent theoretical studies[7g,i] suggest that the BP86 functional is an appropriate choice for calculations on the type of systems under investigation. Geometries for local minima were optimized using the program system TURBOMOLE[10] within the framework of the RI-*J* approximation.[11] Transition states have been optimized using the Gaussian program system[12] and have been characterized by one single imaginary frequency. Main group elements have been described by a split-valence basis set with polarization,[13] and Mn was treated with a valence triple-ζ basis set plus one additional *p*-function[14] (α = 0.12765). The local correlation functional employed within the TURBOMOLE program system is that of Vosko and co-workers,[15] whereas the Gaussian program system utilizes the correlation functional due to Perdew. [16]

(6) Palucki, M.; Finney, N. S.; Pospisil, P. J.; Güler, M. L.; Ishida, T.; Jacobsen, E. N. *J. Am. Chem. Soc.* **1998**, *120*, 948.

(7) (a) Norrby, P.-O.; Linde, C.; Åckermark, B.; *J. Am. Chem. Soc.* **1995**, *117*, 11035. (b) Linde, C.; Åckermark, B.; Norrby, P.-O.; Svensson, M. *J. Am. Chem. Soc.* **1999**, *121*, 5083. (c) Strassner, T.; Houk, K. N. *Org. Lett.* **1999**, *1*, 419. (d) Cavallo, L.; Jacobsen, H. *Angew. Chem.* **2000**, *112*, 602; *Angew. Chem., Int. Ed.* **2000**,*39*, 589. (e) Jacobsen, H.; Cavallo, L. *Chem. Eur. J.* **2001**, *7*, 800. (f) El-Bahraoui, J.; Wiest, O.; Feichtinger, D.; Plattner, D. A. *Angew. Chem.* **2001**, *109*, 1796; *Angew. Chem., Int. Ed.* **2001**,*40*, 2073. (g) Abashkin, Y. G.; Collins, J. R.; Burt, S. K. *Inorg. Chem.* **2001**, *40*, 4040. (h) Cavallo, L.; Jacobsen, H. *Eur. J. Inorg. Chem.* **2003**, 892. (i) Cavallo, L.; Jacobsen, H. *J. Phys. Chem. A* **2003**, *107*, 5466.

(8) Becke, A. D. *Phys. Rev.* **1988**, *A38*, 3098.

(9) Perdew, J. P. *Phys. Rev.* **1986**, *B33*, 8822.

(10) (a) Ahlrichs, R.; Bär, M.; Häser, M.; Horn, H.; Kölmel, C.; *Chem. Phys. Lett.* **1989**, *162*, 165−169. (b) Treutler, O.; Ahlrichs, R. *J. Chem. Phys.* **1995** *102*, 346−354. (c) M. Von Arnim, M.; Ahlrichs, R. *J. Comput. Chem.* **1998** *19*, 1746.

(11) (a) Eichkorn, K.; Treutler, O.; Öhm, H.; Häser, M.; Ahlrichs, R. *Chem. Phys. Lett.* **1995**, *242*, 652−670. (b) Eichkorn, K.; Weigand, F.; Treutler, O.; Ahlrichs, R. *Theor. Chem. Acc.* **1997**, *97*, 119−124.

TABLE 1. Relative Energies (in kJ/mol) of Quintet and Triplet Geometries of (acacen′)Mn^{III} and (salen)Mn^{III} Systems

	2	2a	2b	2c	2d	2e	2f
[^{5}Mn^{III}]	0.0	0.0	0.0	0.0	0.0	0.0	0.0
[^{3}Mn^{III}]	37.8	33.3	35.3	27.3	32.8	30.2	30.0

TABLE 2. Relative Energies (in kJ/mol) of Triplet and Singulet Geometries of (acacen′)Mn^{V} Oxo and (salen)Mn^{V} Oxo Systems

	3	3a	3b	3c	3d	3e	3f
[^{3}Mn^{V}=O]	4.7	0.0	0.0	0.0	0.0	0.0	0.0
[^{1}Mn^{V}=O]	0	3.6	2.3	2.0	3.1	2.3	3.1

Results and Discussion

Electronic Structure of (salen)Mn and (acacen′)-Mn Systems. Several of the previous theoretical studies explore and explain the electronic structure of the (acacen′)Mn^{III} model compound **2**.[7c,d,g] In principle, in its most stable geometry, this complex possesses a square-planar coordination having an electronic quintet configuration, with a triplet state being about 30−40 kJ/mol higher in energy. A singulet state, which is at even higher energies, undergoes a distortion of the square-planar coordination mode of the acacen′ ligand and is therefore in general not considered to be of importance for catalytic epoxidation reactions. The results of the present study are consistent with the earlier observations, and relative energies for quintet and triplet geometries are compiled in Table 1.

Regarding our notation, [^{5}Mn^{III}] stands for the quintet state geometry of a (salen)Mn^{III} or (acacen′)Mn^{III} complex. Singulet and triplet states, as well as oxo complexes, in which the metal center has the formal oxidation state +V, will be designated accordingly. We see that for the (acacen′)Mn^{III} complex **2**, as well as for the (salen)Mn^{III} complexes **2a**−**f**, the quintet state is energetically favored over the triplet state. Interestingly, of all molecules under investigation, the model complex **2** displays the largest quintet-triplet splitting. Compared to the (salen)Mn^{III} complex **2a** with H atoms in 5,5′ position, we note that electron-withdrawing ligands in 5,5′ position, such as NO_2 in complex **2b**, raise the quintet-triplet gap, whereas electron-donating ligands in 5,5′ position, such as OMe in complex **2c**, lower the quintet-triplet gap.

The situation is more interesting for the oxo species **3**. Whereas previous studies all agree that now the quintet state is higher in energy than the triplet state, it is also observed that a singulet state constitutes the most stable system, the triplet, however, being only about 5 kJ/mol higher in energy.[7c,d,g] This observation prompted Abashkin and co-workers to consider an epoxidation profile on the singulet surface,[7g] whereas the observation that other intermediates during the epoxidation reaction have energetically unfavorable singulet states led us to propose an epoxidation scheme under conservation of spin on the triplet surface.[7c] Relative energies for triplet and singulet geometries are compiled in Table 2.

In accord with previous studies, the model complex **3** prefers a singulet state to a triplet state, the triplet being about 5 kJ/mol higher in energy. However, turning to the (salen)Mn^{V} oxo complexes **3a**−**f**, we observe that the extended aromatic system allows for more effective electron delocalization, stabilizing a triplet state relative to a singulet state. Therefore, for complexes **3a**−**f** the triplet constitutes in all cases the most stable state, the singulet being about 3 kJ/mol higher in energy.

Coordination Geometry of the Oxo Species. The optimized geometry of complex **3d** as a representative example for the oxo species under investigation is displayed in Figure 2. The important feature here is that the coordinated salen ligand does not possess a planar coordination mode but is folded with relevant folding angles[7h] φ_+ and φ_-. Values for folding angles are collected in Table 3.

We have argued before that the folded ligand geometry creates a chiral pocket, substantially responsible for chiral induction in the enantioselective epoxidation.[7e] A recent study by Wiest and co-workers on (salen)Mn^{V}-type systems concludes that the axial ligand is responsible for and determines the degree of ligand folding.[7f] The present study suggests that the oxo systems with a chloride ligand in axial position are inherently folded, with substantial fold angles between 155° and 165°.

Correlation of Electronic Properties with Hammett Parameters. Following ideas developed in the context of quantitative structure−properties relationships (QSPR),[17] we now attempt to establish sensible molecular descriptors in order to develop a better understanding of how ligand substitution in 5,5′ position might influence the catalytic activity of (salen)Mn epoxidation catalysts. Since the dawn of QSPR, empirical parameters related to structural and electronic molecular properties have been used as molecular descriptors to determine such relationships. Among all of these parameters, Hammett σ constants[18,19] have been massively employed in QSPR studies. What we are ultimately interested in is the question of how substitution modification of the aromatic system of the coordinated salen ligand influences the reactivity of the oxo ligand. This, in turn, influences the nature of the first transition state for an epoxidation reaction and thus determines the catalytic characteristics as varied by substituent modification. The effects due to variation of the electronic structure of the

(12) Frisch, M. J.; Trucks, G. W.; Schlegel, H. B.; Scuseria, G. E.; Robb, M. A.; Cheeseman, J. R.; Zakrzewski, V. G.; Montgomery, Jr., J. A.; Stratmann, R. E.; Burant, J. C.; Dapprich, S.; Millam, J. M.; Daniels, A. D.; Kudin, K. N.; Strain, M. C.; Farkas, O.; Tomasi, J.; Barone, V.; Cossi, M.; Cammi, R.; Mennucci, B.; Pomelli, C.; Adamo, C.; Clifford, S.; Ochterski, J.; Petersson, G. A.; Ayala, P. Y.; Cui, Q.; Morokuma, K.; Malick, D. K.; Rabuck, A. D.; Raghavachari, K.; Foresman, J. B.; Cioslowski, J.; Ortiz, J. V.; Stefanov, B. B.; Liu, G.; Liashenko, A.; Piskorz, P.; Komaromi, I.; Gomperts, R.; Martin, R. L.; Fox, D. J.; Keith, T.; Al-Laham, M. A.; Peng, C. Y.; Nanayakkara, A.; Gonzalez, C.; Challacombe, M.; Gill, P. M. W.; Johnson, B.; Chen, W.; Wong, M. W.; Andres, J. L.; Gonzalez, C.; Head-Gordon, M.; Replogle, E. S.; Pople, J. A. *Gaussian 98*, Rev. A.5; Gaussian Inc.: Pittsburgh, PA, 1998.

(13) Schäfer, A.; Horn, H.; Ahlrichs, R. *J. Chem. Phys.* **1992**, *97*, 2571.

(14) Schäfer, A.; Huber, C.; Ahlrichs, R. *J. Chem. Phys.* **1994**, *100*, 5829.

(15) Vosko, S. H.; Wilk, L.; Nusair, M. *Can. J. Phys.* **1980**, *58*, 1200−1211.

(16) Perdew, J. P.; Zunger, A. *Phys. Rev. B* **1981**, *23*, 5048.

(17) van de Waterbeemd, H. *Quant. Struct.−Act. Relat.* **1992** ,*11*, 200.

(18) Hansch, C.; Leo, A.; Taft, R. W. *Chem. Rev.* **1991**, *91*, 165.

(19) Leffler, J. E., Grunwald, E. *Rates and Equilibria of Organic Reactions*; Wiley: New York, 1963.

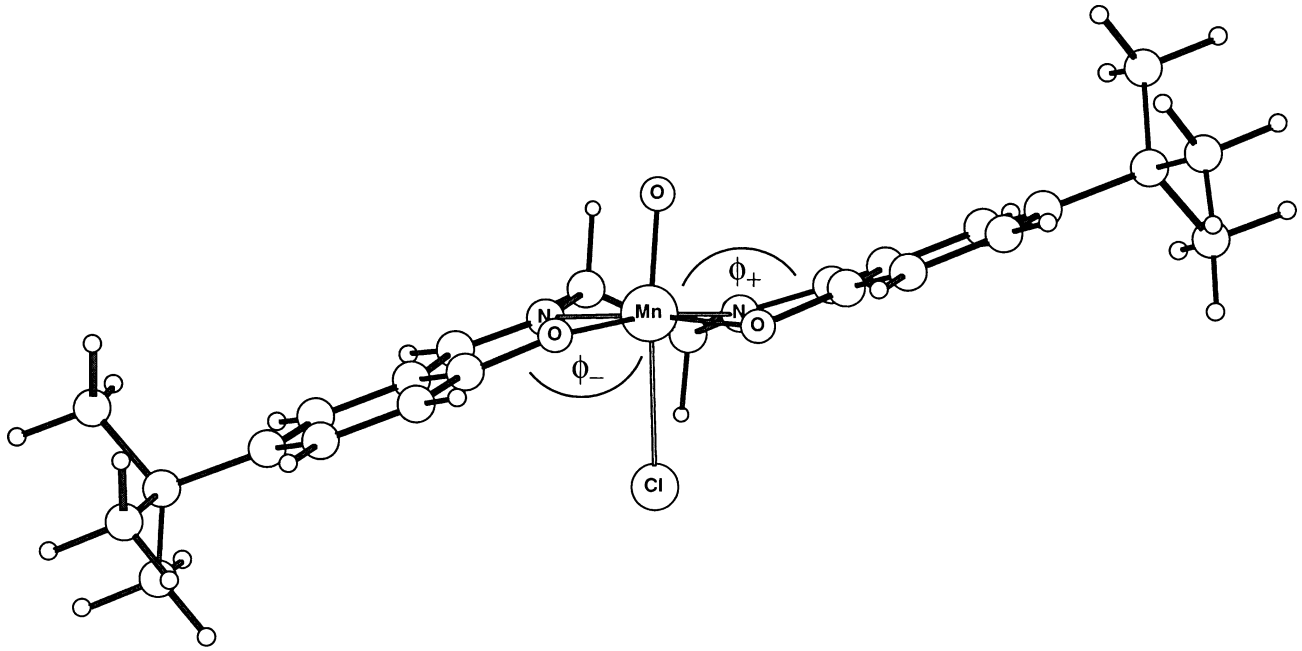

FIGURE 2. Optimized geometry for the (salen)Mn^{V} oxo complex **3d**, having tertiary butyl groups in 5,5′ position of the salen ligand.

TABLE 3. Fold Angles (in deg) for Optimized Triplet Geometries of (acacen′)Mn^{V} Oxo and (salen)Mn^{V} Oxo Systems

	3	3a	3b	3c	3d	3e	3f
φ_+	160	156	157	155	155	156	156
φ_-	164	165	164	165	165	165	165

aromatic system under substituent modification are to be transferred to the oxo ligand via the manganese transition metal center. Therefore, modifications in aromatic substitution might be classified as to correspond to a secondary substituent effect. In the following, we are going to use modified Hammett constants σ^{+}_{para}, the so-called electrophilic substituent constants, to establish correlation relationships. The modified Hammett constants account for electron resonance and through conjugation effects,[18] which are of importance when characterizing a secondary substituent effect.

In Figure 3, a correlation between σ^{+}_{para} and Mulliken charges at the oxo ligand q_{Oxo} for the (salen)Mn^{V} oxo complexes **3a**−**f** is presented.

As might have been expected, electron-donating substituents such as OMe cause an increase of negative charge at the oxo ligand, whereas electron-withdrawing substituents such as NO_2 cause the opposite effect. We note that the q_{Oxo} values correlate reasonably well with the modified Hammett constants. A similar correlation was found for partial charges at the oxo ligand derived from other partitioning schemes, such as a population analysis based on occupation numbers, including multicenter corrections.[20]

In Figure 4, a correlation between σ^{+}_{para} and a relative Mn═O bond strength ΔE_{Ox} is shown.

(20) (a) Heinzmann, R.; Ahlrichs, R. *Theor. Chim. Acta* **1976**, *42*, 33. (b) Ehrhardt, C.; Ahlrichs, R. *Theor. Chim. Acta* **1985**, *68*, 231.

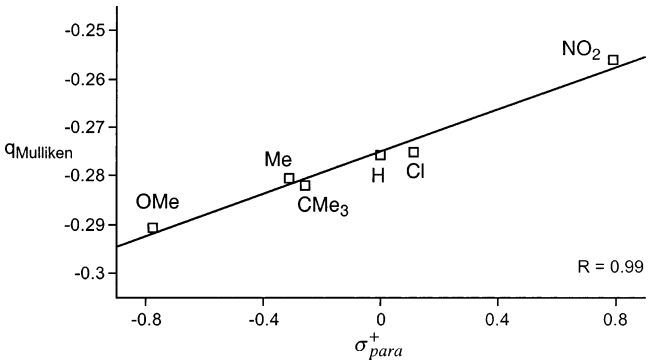

FIGURE 3. Correlation of modified Hammet constants σ^{+}_{para} for the 5,5-substituents in the oxo complexes **3a**−**f** with Mulliken charges q_{Oxo} (in au) at the oxo ligand (σ^{+}_{para} values from ref 19).

The values for ΔE_{Ox} have been derived from the following hypothetical reaction

$$2[^5Mn^{III}] + {}^3O_2 \rightarrow 2[^3Mn^{V}{=}O] \quad (1)$$

and have been calculated as

$$\Delta E_{Ox} = 2E([^3Mn^{V}{=}O]) - 2E([^5Mn^{III}]) - E(^3O_2) \quad (2)$$

One can deduce from Figure 4 that electron-donating substituents cause a stronger Mn═O bond, whereas electron-withdrawing substituents give rise to a weaker Mn═O bond. The difference in Mn═O bond strength for the prototypical donor and acceptor substituents OMe and NO_2 amounts to roughly 20 kJ/mol. Again, we note that ΔE_{Ox} correlates favorably with σ^{+}_{para}.

The correlation shown in Figure 3 is consistent with the electronic picture developed for oxygen transfer reactions mediated by the low valent transition metal oxo

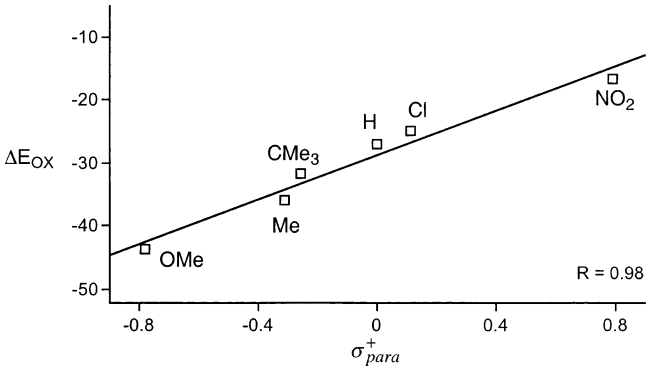

FIGURE 4. Correlation of modified Hammett constants σ^{+}_{para} for the 5,5-substituents in the oxo complexes **3a**−**f** with ΔE_{Ox} values (ΔE_{Ox} in kJ/mol, σ^{+}_{para} values from ref 19).

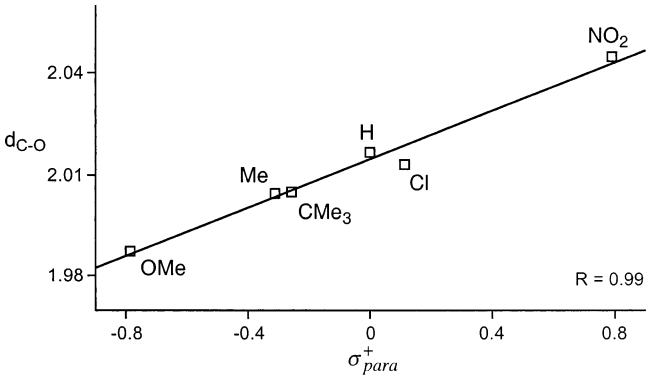

FIGURE 5. Correlation of modified Hammett constants σ^{+}_{para} for the 5,5-substituents in the transition states **4a**−**f** with d_{C-O} values (in Å) for the evolving carbon−oxygen bond (σ^{+}_{para} values from ref 19).

complexes $ReO(O_2)_2(CH_3)$ and $Mo(O)(O_2)_2(OPR_3)$,[21] as well as (acacen′)(O)Mn.[7h] Charge and orbital analyses performed for the transition state of ethylene oxidation suggest that the oxidation reaction is to be classified as electrophilic attack of the oxo ligand at the olefinic double bond. It is to be expected that the smaller the amount of negative charge at the oxo ligand the more favored the electrophilic attack at the HOMO of the olefinic system. Therefore, systems with a smaller amount of negative charge at the oxo center should result in an earlier, more educt-like transition state, whereas systems with a larger amount of negative charge at the oxo center should result in a later, more product-like transition state. The same conclusion can be drawn from the correlation in Figure 4, which suggests that the first step of the epoxidation reaction is energetically controlled. Here, the amount of bond breaking, formally required in reduction of the Mn−O bond order when going from the Mn^{V} oxo species to the Mn^{IV} radical intermediate, determines the position of the transition state. Again, it is to be expected that systems with electron-withdrawing substituents and possessing weak Mn═O bonds should react in an earlier, more educt-like transition state, whereas systems with electron-donating substituents and possessing strong Mn═O bonds should react in a later, more product-like transition state.

Correlation of Transition State Geometries with Hammett Parameters. To further substantiate the influence of substitution at the salen ligand framework on the course of the epoxidation reaction, we optimized the transition states geometries for the first C−O bond formation **4a**−**f**.

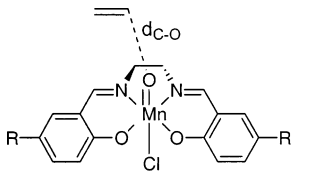

4a: R = H
4b: R = NO_2
4c: R = OMe
4d: R = CMe_3
4e: R = Cl
4f : R = Me

The reaction profile for epoxide formation is expected to proceed through first and second transition states, which correspond to formation of the first and second C−O bond, respectively. However, it is the first transition state in which the enantioselectivity is determined, since it is the first transition state leading to the formation of the first chiral carbon atom. Although because of the simplified nature of the model compounds used, no chiral carbon atom is actually present in the set of model compounds employed, it is a reasonable assumption that the results presented here allow one to make valid analogy conclusions for the real system. We refer the reader to the literature[7e] for a detailed discussion on the aspect of enantioselectivity from a theoretical point of view. The second transition state could be determining for the overall reaction rate, for the distribution ratio of *cis*/*trans* products, but not for the ee value of the epoxidation reaction, which often represents the sensible data by which the performance of a catalyst for chiral epoxidation is judged.

Our previous studies have already elucidated the importance of the first C−O bond formation as essential mechanistic step in the epoxidation reaction.[7d,e,h] Depending on the nature of the salen ligand, distances for the evolving C−O bond d_{C-O} range from 1.98 to 2.05 Å. Turning now to Figure 5, a correlation between σ^{+}_{para} and d_{C-O} values is displayed.

This favorable correlation illustrates the influence exerted by the substitutents of the salen ligand on the geometries of the first C−O bond-forming transition states and essentially confirms the previously suggested mechanistic picture. Referring back to Figure 1, the reaction coordinate along which the first transition states occurs correlates with the distance between the atoms involved in formation of the new C−O bond, and systems with electron-withdrawing substituents react in an earlier, more educt-like transition state, whereas systems with electron-donating substituents react in a later, more product-like transition state. The same conclusion is drawn when analyzing the d_{C-O} values for the various transition state geometries as reported in Figure 5. Systems with electron withdrawing substituents show a longer C−O separation than systems with electron-donating substituents.

(21) Deubel, D. V.; Frenking, G.; Senn, H. M.; Sundermeyer, J. *Chem. Commun.* **2000**, 2469.

The detailed investigation by Jacobsen and co-workers[6] reveals that linear Hammett plots correlate enantioselectivity in the epoxidation of olefins with Hammett values of the 5,5′-substituents on the catalyst, and furthermore that enantioselectivity in epoxidation with the most selective catalysts relies almost entirely on enthalpic factors. The following considerations tie the d_{C-O} values to degree of enantioselectivity. A late transition state requires a certain proximity between the olefin and the manganese oxo complex. This leads to a lesser amount of spatial separation between substrate and catalyst and concomitantly to enhanced differentiation of diastereomeric transition structures.[22] A computational case study has already analyzed the subtle effects that come into play when possible transition state geometries are analyzed.[7e] Enantioselectivity is governed by interactions of the salen ligand, which in the transition state geometry adapts a folded geometry forming a chiral pocket, and the incoming olefin. These interactions in turn are highly dependent on the value of d_{C-O}.

In light of the previously discussed results (compare Figure 4), the present theoretical work suggests that the electronic influence of the 5,5′-substituents manifests itself in a tuning of the Mn═O bond strength. Systems with a stronger Mn═O bond require a larger amount of activation energy and therefore react in a relatively late transition state. The value for d_{C-O} together with the Mn═O bond strength holds an explanation for the experimental result that enantioselectivity in epoxidation relies almost entirely on enthalpic factors.

(22) Lipkowitz, K. B.; D'Hue, C. A.; Sakamoto, T.; Stack, J. N. *J. Am. Chem. Soc.* **2002**, *124*, 14255.

Conclusion

The present study demonstrates that the current density functional methods allow for a successful correlation of computed properties with experimental values in the context of the transition-metal-catalyzed epoxidation of olefins, even for computational challenging systems such as the (salen)Mn catalysts investigated here. These encouraging results might have implications in the analysis of quantitative structure−activity relationships. The notion that enantioselectivity is tied to the position of a transition state along the reaction coordinate is supported in the current work. Electronic effects exhibited by the 5,5′ substituents of the catalyst manifest themselves in a tuning of the Mn═O bond strength.

Acknowledgment. Università di Salerno and MURST of Italy generously supported the present work. Access to the computational facilities at ACI, Universität Zürich, is gratefully acknowledged. The authors thank CIMCF of the Università Federico II of Naples for technical assistance and professor T. K. Woo of the University of Western Ontario and the Sharcnet project for generous access to computer resources.

Supporting Information Available: Listing of Cartesian coordinates and final energies for all optimized geometries, as well as imaginary frequencies for transition states. This material is available free of charge via the Internet at http://pubs.acs.org.

JO034059A